https://doi.org/10.2352/ISSN.2169-4451.2017.32.60

Measurement of Inkjet Printhead Reliability by Detecting Every Single Droplet in Flight

Ingo Reinhold,[1,2] Tomáš Černý,[3] Maik Müller,[1] Werner Zapka[1]; [1]XaarJet AB, Järfälla, Sweden, [2]Industrial and Medical Electronics, Royal Institute of Technology (KTH), Stockholm, Sweden, [3]Xaar plc, Cambridge, UK

Abstract

Inkjet printing is adapted for many digital imaging systems including graphical, industrial and advanced manufacturing applications. Reliability was identified to be one of the key challenges for inkjet printheads due to their susceptibility to variations in temperature, ink consistency, debris or external vibration. Hence, lengthy tests with printouts on kilometers of papers are necessary to establish a measure of reliability, which is time-consuming and extends the development cycle for a given application.

In this contribution a line-scan camera is used to observe all droplets from a printhead row in flight at full jetting frequency. This allows for the identification of missing droplets as a function of the printed image, external disturbances as well as the drive waveforms used and other print parameters. This provides a quantitative measurement not only of reliability but also of deviations in droplet velocity and trajectory in a laboratory environment. The paper discusses the necessary hard- and software approaches and details the necessity for various image transformations due to the challenges imposed by the illumination. Furthermore, we will present experimental data as well as speed benchmarks.

Introduction

Reliability is one of the key challenges in inkjet technology. Nozzles perform unreliably for a number of reasons, such as intermediate drying, ingestion of air, print system vibration, nozzle plate flooding, clogging through air- and ink-borne contaminants. These faults partially result from the design of the printing system but are mainly related to the intrinsic operation of the printhead, where crosstalk, temperature differences and water hammer phenomena may compromise the stability of the ink-printhead combination. Development of highly sophisticated drive waveforms is therefore necessary to ensure good droplet formation, which is characterized by high droplet velocities and low satellite count. At the same time swift restoration of the initial state of the channel is needed for reproducible and consistent operation.

Nozzle outages in the field are more easily assessable by visual inspection, but the measurement capability during waveform optimization is challenging, as droplet formation studies are typically performed using stroboscopic imaging techniques with a restricted field of view. Laboratory print tests are elaborate, consume large amounts of ink and paper and are often visually inspected by humans, which provide a rather qualitative picture of reliability. Nozzle outages in addition are often only a temporary phenomenon, which may recover for instance by the dissolution of an air bubble into the ink or, in the case of printheads using convective/recirculating flow, by removal of the disturbance from the channel.

Channel health monitoring is broadly discussed in the literature. Insights can be retrieved from monitoring the acoustics in the channel [1] or the motion of the meniscus inside the nozzle,[2] which give a good indication for the adequate performance of the printhead but are merely indirect measures of droplet formation. More insight may be gained by observing the trajectory of a droplet detached from the nozzle, which may be achieved by light scattering[3] or grey level analysis in superimposed images from area scan cameras.[4] These techniques, however, only have limited applicability for self-recovering printheads as the analysis is often limited to a few nozzles or does not resolve every single droplet.

In this contribution we demonstrate a system to analyze complete rows of printheads using a line-scan camera and accompanying software-based preconditioning approach. Theoretical aspects of the system and the resulting implications for the need for preconditioning are discussed, followed by an overview of the software approach alongside with results from images taken with a Xaar1002-type printhead.

Measurement Principle

Observing all nozzles from a row of nozzles on a printhead presents a bandwidth issue, as traditional laboratory imaging techniques such as stroboscopic illumination or high-speed camera imaging generate a tremendous amount of data, which is not necessary for gathering information about the presence of a droplet from a given nozzle at a given time. The chosen approach using a line-scan camera elegantly reduces the amount of data by integrating the shadow of a passing droplet into a single pixel, which can be equated to time. In addition, the lateral resolution of a line-scan camera is sufficient to record shadowing effects with a number of pixels per nozzle allowing for the discrimination of droplets and background. The combination of sufficient resolution across the printhead and line-readout frequencies in the kilohertz range allow for monitoring of all nozzles at jetting frequency.

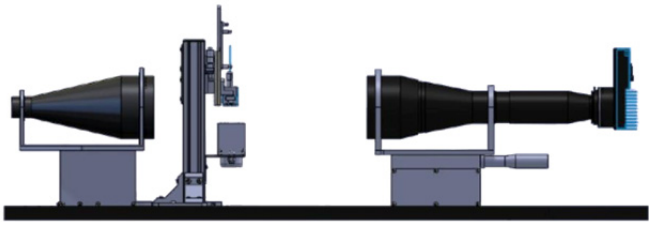

Figure 1: Schematic of the experimental setup using a telecentric illuminator, a printhead holder with an accompanying ink collector and a demagnifying telecentric optic that images the droplet onto the CMOS sensor of a line scan camera (left to right).

To ensure capturing of all the ejection events, oversampling is required. In case of three-cycle operation as for the Xaar1002, oversampling is naturally provided if one chooses the camera frequency equal to the cycle frequency. Furthermore, the resulting contrast has to be considered, as a droplet may be passing through the camera's field of view of 20 µm with a velocity of 5 ms^{-1} or higher. The 4 µs during which the droplet casts a shadow onto the image sensor account only for 10% of the integration time of the camera when running the printhead at 6 kHz. Hence, a constant instead of a pulsed illumination is chosen as this will guarantee the capturing of every printed droplet irrespective of its variation in drop velocity resulting from crosstalk, misalignment and waveform. The camera then

can be set to record frames back-to-back with a near zero dead time.

A simple model using boxcar functions to represent droplet size, field of view as well as the exposure time of the camera[5] was applied to further understand the greylevel distribution of the resulting recorded images.

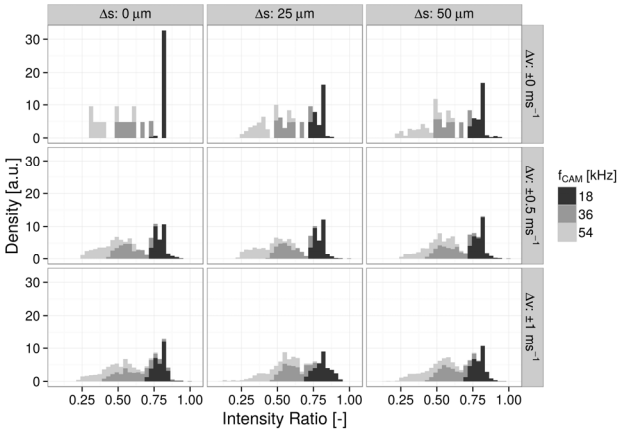

Figure 2: Theoretical greygrey level distributions in imaging of droplets of seven different droplet volumes at different camera frequencies [stacked histogram, nominal droplet velocity 6 ms^{-1}, sensor distance to nozzle plate 250 µm from the nozzle plate, sub-droplet size: 6 pL, Δs variation in starting position, Δv variation in drop velocity].

Figure 2 presents results of a simulation where the camera frequency and hence the exposure time was varied between 18 and 54 kHz. The achieved greylevels generated by the droplet passing the camera are in the range of 80% for the lower oversampling rate of 18 kHz. This is improved with higher sampling rates due to the decrease in illumination times, but show larger spread due to the double exposure of pixels by the same droplet and hence distribution of the shadow onto two neighboring pixels in time, which results in a greylevel closer to that of the background illumination.

This very simplified assessment highlights the challenge of a reduced contrast and shows that the three-fold oversample, i.e. using a camera frequency of 18 kHz with a line frequency of the printhead of 6 kHz, presents a good compromise between data rate and discrimination of the droplet, where the droplet size as well as the variations have a less pronounced effect on variation of the grey level.

Image Analysis

Quantitative analysis of these recorded images needs to robustly discriminate between the back- and the foreground pixels, and to deal with the variations outlined above. Therefore an area of interest (AOI) was used which spans both dimensions of the image data, namely time to compensate for the velocity variation as well as laterally to adapt for variations in trajectory. The test pattern, which was printed, was hereby used to provide the location of the center of the AOI and to extrapolate for the resulting image characteristics.

The detection of a droplet present in the desired AOI was performed by using binarization and a respective threshold. Thresholding presents a key challenge in image processing and is also critical in this present context, as the low contrast of the images in conjunction with the varying droplet sizes, different photon responses of the different camera pixels and droplets arriving between the exposures of two subsequent lines. The Gaussians representing the droplet as well as the background are located relatively close to each other and are difficult to deconvolute.

The following approaches have been taken to improve the selectivity of the automated process and enable detection of single droplets in the recorded images. For a more detailed view on the used techniques we refer the interested reader to *Zapka et al.*[5]

Contrast Optimization

After an initial erosion step (*cf.* Figure 3 (Erode)) a linear histogram stretching is performed to increase the detectability of the two convoluted distributions. In this computation one needs to bear in mind that some of the 39 million pixels analyzed per image originate from slowly traveling droplets or bright pixels from an erroneous flat-field correction of the camera. The limits used for generating the look-up-table (LUT) for the stretch conversion are hence chosen in such a fashion that these artifacts are compressed into the standard droplet and background distributions while preserving the overall characteristics of the distribution.

Figure 3 (Stretch) visualizes a typical histogram after the application of such a LUT. It clearly shows that there is an additional maximum at a grey level of 136 in the background data. This stems from droplets being present in two subsequent pixels by being incorrectly timed through altered starting times or droplet velocities. As a result this additional maximum is to be expected in all of the histograms.

Finally, another histogram based transformation is applied, which combines the knowledge of the location of droplets in the image with techniques known for histogram equalization. We anticipate here that histograms are simply a summation of the two Gaussian distributions for the droplets (D) and the background (B). By analyzing the image the characteristics, such as average and standard deviation can be measured. From histogram equalization we can calculate the cumulative distribution function (CDF). In order to separate these two Gaussians, two desired distributions can be prescribed based on the source distributions. Matching up the two resulting CDFs by a nearest neighbour approach allows for the histogram-matching transformation, which yields Figure 3 (Match).

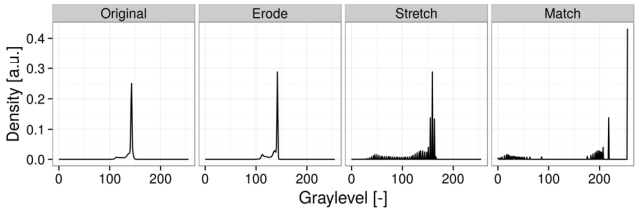

Figure 3: Change of the histograms in the course of the pre-processing from original, after erosion with a linear filter element, low contrast optimization and histogram matching.

Figure 3 (Match) clearly shows the success of the deconvolution without intermediate pixels values and hence a robust outset for a thresholding operation. Overviews of image pixel results from all transformations applied are presented in Figure 4. The improvement in contrast without the generation of artefacts is clearly visible from this representation.

Using the outcome of the discussed preflight techniques, an analysis can be conducted that uses the recorded images as well as the 'pattern to be printed' and encodes the results using grey levels into an image corresponding to the dimensions of the original print pattern.

As outlined above, the detection of the droplet is accomplished by comparing a characteristic value of the AOI to a threshold value. The threshold value is calculated from the histogram after the matching transformation. The calculation of this characteristic value may be accomplished by numerous techniques such as averaging, minimum and maximum

determination, standard errors, morphology, etc. The simplest implementation presented here is the use of the minimum grey value inside the AOI. In this sense a droplet is marked as present if the minimum value is lower than the threshold. Otherwise the pixel is marked as *missing* in the results matrix.

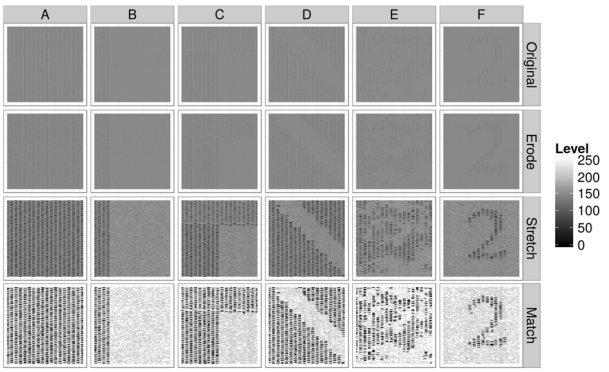

Figure 4: Image representations for six selected areas of the test image at different stages of the used algorithms: (1) Original, (2) Eroded with kernel size 3, (3) Stretched histogram with the limits [104, 167], (4) Histogram matching with s1=0.3, μ1=0.5, σ1=1, s2=0.6, μ2=1.5, σ2=1 [Xaar1002GS40, 6 kHz printhead frequency].

The presence of a minimum lower than the threshold, however, does not necessarily indicate the presence of a printed droplet, as other factors such as mist and neighbouring missing channels may spray into the trajectory of the droplet under consideration. Additional examinations of the AOI statistics are necessary in order to discriminate these. Disturbances such as failing neighbour channels and spraying typically result in fully darkened AOI, which dramatically change the statistics. As a result these AOIs are marked as *untrusted*, as insufficient information is available to assess its state.

In addition, the lateral distribution of the pixel grey levels can be used to provide qualitative information about the droplet such as excessive droplet velocity variation or trajectory deviation.

Experimental Results

Figure 5 shows a compilation of the analysis results from a small portion of a single image of a test run using the print pattern shown in (a). In order to provoke misbehaviour of the printhead and thus to provide a sufficient amount of drop formation failures, a detuned drive waveform was used. Figure 5 (b) is the encoded image as it is output from the analysis program, giving a rough overview of all the defects observed. Figure 5 (c) shows the detected missing droplets, which clearly originate from a single nozzle that failed for a certain time duration, recovered and then repeatedly failed again, which would thus produce a series of 'tic' marks in a printout. Since all other nozzles with similar drive conditions show no issues, the failure is most likely due to debris at the nozzle, which dislocates and returns to the nozzle in the course of time. Figure 5 (d) shows 'ghost' droplets, which are droplets found in a supposedly white space in the image. When overlaying these images with the original print pattern, it becomes evident that all of these are located one pixel after the lowest grey level is printed. Obviously these ghost drops are droplets delayed due to a strongly reduced droplet velocity and susceptibility to air motion. Figure 5 (e) shows the untrusted AOIs where double exposure or airborne impurities are to be found. These are mainly observed in the vicinity of a failing channel as well as for low volume drops, where droplet velocity is insufficient to sustain straight trajectories. Figure 5 (f) and (g) highlight the capability of the LineScan technique, to give qualitative information about droplet velocity. Figure (f) shows those droplets which appear to have an excessive drop velocity. These show up predominantly in the areas around the failing nozzles, which may result from the changed acoustics and crosstalk in the vicinity of misfiring channels. Figure 5 (g) shows droplets which are considered too slow. It is evident that there is some velocity ringing in the initial stage of printing the image, which shows the extensive? detail the presented approach can provide.

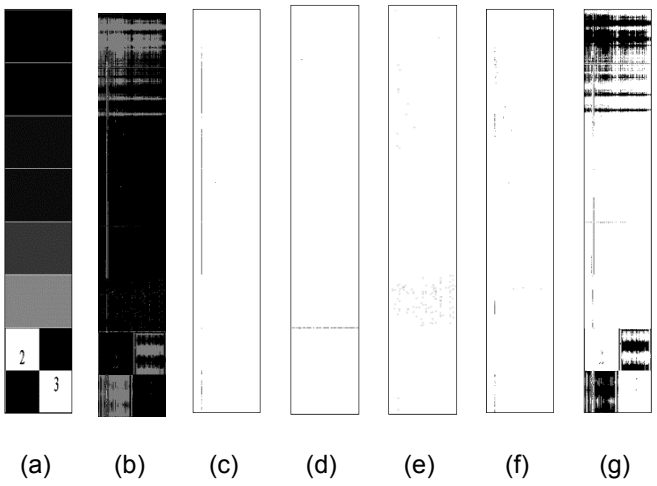

Figure 5: Print pattern and the results of the analysis: (a) original pattern, (b) composite result, (c) missing pixels, (d) ghost droplets, (e) untrusted AOIs, (f) fast droplets, (g) slow droplets.

The numerical results of the images in Figure 5 can then be used to analyze overall *tic mark* length by using a hypothetical print resolution. Figure 6 shows such a summary for a printhead at 6 kHz print frequency and printing at 360 dpi hypothetical print resolution. The *tic marks* in this case are clustered to 1 mm in length. It is evident that the developed LineScan algorithm is capable of detecting not only relatively short tics but also nozzles failing for a much longer period, such as nozzles, which do not recover, e.g. due to influences like nozzle clogging.

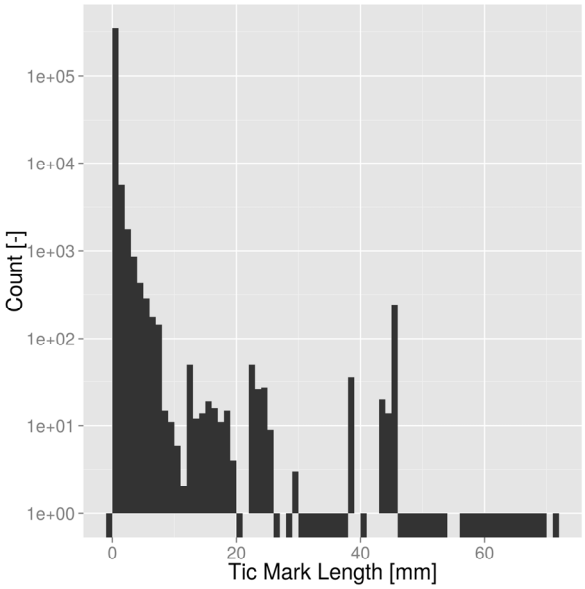

Figure 6: Histogram of the detected tic marks in an experiment of five minutes continuous jetting at 6 kHz with a detuned waveform [bin width 1 mm].

The amount of short tic marks is surprising but needs to be related to the failure mechanisms. Such failure mechanisms are mainly attributed to the detuned waveform used, and hint at certain nozzles restarting after a single misfire potentially due to a combination of actuations of neighbouring channels before either normal operation is restored or the failure manifests itself in a longer tic mark. It could furthermore relate to the ingestion of a small air bubble resulting from the destabilization of the ink meniscus in the nozzle or a flooded nozzle plate. For a hybrid side shooter printhead with maximum throughflow velocity of 1 ms^{-1} in the center of the channel, the removal of an ingested air bubble will disturb the acoustics of a channel for roughly 1 ms, which corresponds to the failing of six subsequent ejections. This may explain the cause of tic marks of length of roughly half a millimeter.

More thorough investigations are, however, required to understand the nature of the observed distributions fully.

Performance

Performance is a key challenge for such an application. Online monitoring, i.e. performing the recording and analysis in real time, is challenging due to the relatively large amount of data to be processed. The use of programming languages including their low-level features is meant to gain speed and enable efficient processing. Furthermore, the transfer of the algorithms to dedicated parallel-processing hardware as it is often observed for machine vision applications is a further possibility.

The results presented were implemented in C++ with partially parallel structures. The implementation allows for processing times, excluding the recording and writing times of images, of roughly 450 ms for a single capture image of 10668 lines on a Dell Optiplex 9010. This corresponds to 75% of the frame rate of the camera at 18 kHz line rate. Hence, with sufficiently efficient memory transfer concepts, this may already present the possibility for real-time processing.

Conclusion and Outlook

We have presented a system to analyze the ejection of every single droplet from a printhead row using a constant illumination. A simple mathematical model was used to gain insight into the grey level distributions, which can be expected from the recording hardware. The results show that simple oversampling offers the best trade-off between data rates and contrast. The contrast in the system is expected to be rather low, as the residence time of the droplet in front of the camera is short compared to the integration time of the camera.

In order to improve the contrast a set of preconditioning image transformations are proposed, which include erosion, histogram stretching as well as histogram matching. The knowledge of the pixel positions was used to deconvolute the information of the Gaussian distributions from the droplets and the background.

A threshold based approach was used to detect the presence of a droplet. Additional information derived from the distributions of the grey levels in the area of interest AOI allowed for qualitative analysis of velocity as well as the trajectory of the droplet.

While the current implementation of the line-scan technique allows for the real-time analysis of the acquired images, future work will concentrate on further optimization of these algorithms. Furthermore, the interpretation of the results due to the complexity of the failure mechanisms of a nozzle is still immature and requires further attention.

References

[1] S. Koekebakker, M. Ezzeldin, A. Khalate, R. Babuška, X. Bombois, P. van den Bosch, G. Scorletti, S. Weiland, H. Wijshoff, R. Waarsing, and W. de Zeeuw, "Piezo Printhead Control: Jetting Any Drop at Any Time," in Model-Based Design of Adaptive Embedded Systems, Embedded Systems, vol. 22, 2013, pp. 41–85.

[2] J. Wei, C. Yue, G. Zhang, P. M. Sarro, and J. F. Dijksman, "Monitoring of Meniscus Motion at Nozzle Orifice with Capacitive Sensor for Inkjet Applications," in IEEE Sensors, 2012, pp. 1–4.

[3] J. L. Valero and L. Portela, "HP Inkjet Large Format Page Wide Array: Solution for Drop," in International Conference on Non-Impact Printing and Digital Fabrication, 2015, pp. 336–341.

[4] J. Renner, "Real-time Process Monitoring of DoD Inkjet Systems by Overlaid Imaging," in The Inkjet Conference, 2015.

[5] Zapka, W. (Ed.). (*in preparation*). Handbook of Industrial Inkjet Printing. Wiley-VCH.

Author Biography

Ingo Reinhold graduated in micromechanics-mechatronics with emphasis on print- and media technology from Chemnitz University of Technology in 2008. After joining Xaar's Advanced Application Technology group in Stockholm, Sweden, he focused on advanced acoustic driving of piezo-type inkjet printheads alongside with pre- and post-processing of functional materials in digital fabrication. He is currently enrolled as a PhD student within Industrial and Medical Electronics (IME) at the Royal Institute of Technology (KTH) in Stockholm, Sweden.